Non-subjective spatial and temporal evolution of damage following spinal cord injury: Automated and semi-automated recognition of affected areas observed in q-space MR maps

R. Nossin-Manor[1,2], and Y. Cohen[1]

[1]School of Chemistry, Raymond and Beverly Sackler Faculty of Exact Sciences, Tel-Aviv University, Tel-Aviv, Israel, [2]Diagnostic Imaging, The Hospital for Sick Children, Toronto, ON, Canada

Introduction

Quantification of spinal cord damage following trauma is difficult. In the past, we have demonstrated the utility of using high b-value q-space diffusion-weighted MRI to follow the spatial and temporal damage evolution after spinal cord hemi-crush injury [1,2]. In these studies spinal cords were assigned according to their unilateral trauma severity. The spinal cord were removed and fixed 5 days, 10 days and 6 weeks after hemi-crush injury and scanned by MRI using heavily diffusion-weighted imaging. Damage was evaluated using a user-defined procedure [2]. Here we preset automated and semi-automated recognition methods to obtain non-subjective spatial and temporal evolution of the damage following spinal cord injury (SCI).

Methods

Thirty-six male adult Sprague-Dawley rats were subjected to a mild (15 sec) or severe (60 sec) unilateral spinal cord crush. The injury, tissue preparation and MRI protocols were described previously [1,2]. Briefly, in-vitro MRI experiments were performed on post-fixed excised rat's spinal cords 5 days, 10 days and 6 weeks after hemi-crush induction using an 8.4T NMR spectrometer equipped with a micro5-imaging probe (Bruker, Karlshruhe, Germany). The MRI protocol included acquisition of T_1 (TR/TE=500/13ms) and heavily diffusion-weighted images (TR/TE/Δ/δ=2000/20/150/2ms). All images were acquired as 256/128 pixel matrices and were transformed to 256X 256 matrices after FT. First, a sagittal T_1 image was collected to allow selection of five axial 2mm slices with a 1mm gap between them and FOV of 1.5x1.5 cm. Subsequently, diffusion-weighted images were acquired perpendicular to the long axis of the spinal cord. To compute q-space images, sixteen axial heavily diffusion-weighted images were acquired using a stimulated-echo diffusion pulse sequence. Diffusion gradient strength was incremented from 0 to 150 g/cm in 16 steps. Therefore, the maximal b and q values used in these experiments were $1x10^7$ s cm^{-2} and 1277 cm^{-1}, respectively. The q-space MR images were obtained by previously described procedure [1-3]. A 3D array (256x256x16) was arranged from 16 diffusion-weighted images, acquired with linearly increasing q values in a way that the x and y coordinates are the image axes and the z direction is that of the q values. The signal decay in each pixel of the 256x256 matrix was transformed into displacement distribution profiles by a Fourier transformation of the signal decay with respect to q using an in-house Matlab ® program [3]. Two parameters were used to characterize these pixel-by-pixel displacement distribution profiles; namely, the mean displacement and the probability of zero displacement. Finally, the program was used to extract these two parameters on a pixel-by-pixel basis and construct two sub-images referred to as q-space displacement and probability MR maps.

To analyze damage evolution a previously published concept [4] was used to construct a new Matlab program, which was designed to quantify the extent of damage in the acquired slices. To evaluate injury severity as a function of the distance from the trauma site and time following injury, a damage index (DI) was defined by the following expression: DI = (1-NInt)*(LA/TSCA)*100, where NInt is the normalized intensity (i.e., the mean intensity of the unilateral lesion divided by the mean intensity of a normal contra-lateral area), LA is the lesion area and TSCA is the total spinal cord area. Using Matlab, the probability MR maps were processed to calculate the TSCA automatically, and select the LA. Finally, the normalized intensity, NInt, was calculated by dividing the matching lesion probability by the probability of the non-injured contra-lateral side, and DI was determined. The LA was chosen by user-defined, automated and semi-automated recognition of affected areas. The user-defined visual inspection was designed to allow the user straightforward selection of the injured WM tissue by drawing a closed shape around the low probability region. In the automated recognition method, the probability MR maps (Fig. 1a-i) were processed to locate "patches" that corresponded to low probability areas characteristic of the damaged tissue. Using a derivative operator on probability and displacement MR maps, a non user-defined threshold was found for each of them. Then, the program constructed two matching binary images (Fig. 1a-ii and iii, respectively), in which probability (p) and displacement (d) values higher than threshold values were assigned the value 1 (white). These two images were superimposed into one binary image, which was further processed by inverting its polarity (Fig. 1a-iv). Isolated points were then removed using a median filter, and the resulting "patches" were labeled (Fig. 1a-v). "Patch" areas were calculated and the "patch" with the largest area was designated the LA (Fig. 1a-vi). The need for a semi-automated procedure to determine LA arose in cases where injured WM could not be distinguished from GM due to their similar probability values (Fig. 1b-i). The semi-automated recognition method followed the same steps as the automated one (Figs. 1a-ii to iv). Here, however, the user could choose the LA by selecting the low probability area or part of it out of all "patches" regardless of its area (Fig. 1b-v).

Results and Discussion

The automated and semi-automated recognition programs best characterized and quantified the damage at the insult location itself. However, 5 days post mild and severe hemi-crush injuries these two methods had difficulties in recognizing the lesion in rostral and caudal slices further away from the trauma site. This was most likely due to changes observed in the non-injured contra-lateral side of the SC, which possibly reflect edema or reversible secondary processes [4]. Furthermore, as appose to the semi-automated, the automated recognition failed to detect injured WM areas in rostral slices 6 weeks post mild hemi-crush injury. Six weeks after severe hemi-crush injury, however, all three recognition alternatives detected the injured areas and provided full data sets for all 5 slices acquired. Moreover, all three recognition methods showed the same spatial damage evolution. In cases where all three Matlab programs quantified the damage, we found no significant difference in calculated DI values. Nevertheless, DI obtained at the insult location by the automated analyses appeared larger than DI obtained by the user-defined and semi-automated analyses, which provided similar results. The automated procedure overestimated the damage by including normal GM areas in the selected LA, due to the similar probability values of injured WM and normal GM regions. Nevertheless, it is important to note that at the trauma site, all three methods showed the same temporal evolution of the damage indicating spontaneous recovery 6 weeks following mild hemi-crush injury. Consequently, it seems that the automated and semi-automated recognition methods may be suitable for detection of damage at the insult location 5 days and 6 weeks following mild and severe hemi-crush injuries, and for obtaining the spatial damage evolution 6 weeks post-severe trauma. The semi-automated recognition can also be utilized to detect the damage at all 5 slices acquired 6 weeks post-mild trauma. The major advantage of using these recognition procedures is that they consume less time and provide a non-subjective and reproducible outcome.

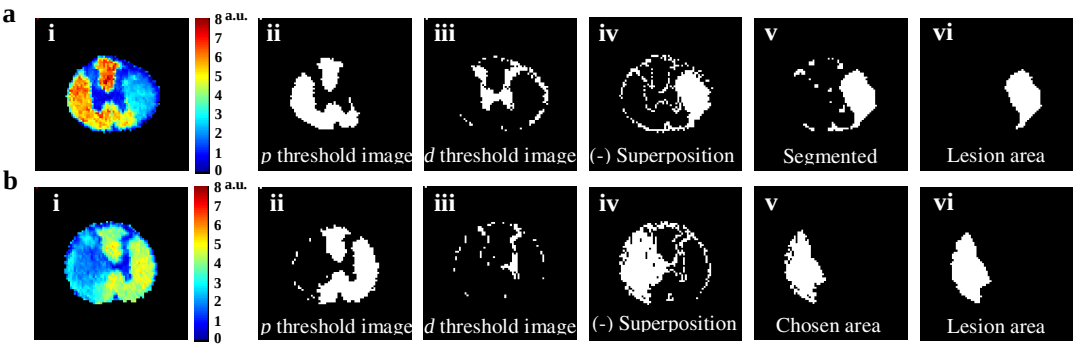

References

1. Nossin-Manor R, et al., Magn. Reson. Imaging 2002**,** 20, 231-241.
2. Nossin-Manor R, et al., J. Neurotrauma 2007, 24, 481-491.
3. Assaf et al., Magn. Reson. Med. 2000, 44**,** 713-722.
4. Kipnis J., et al., J. Neurotrauma 2003, 20, 559-569.

Figure 1: The Automatic (a) and Semi-automatic (b) lesion recognition of affected area (ii – vi) along with the original probability map (i).